

# Emergent light crystal from frustration and pump engineering

Matteo Biondi, Gianni Blatter, and Sebastian Schmidt

*Institute for Theoretical Physics, ETH Zurich, 8093 Zürich, Switzerland*

We demonstrate how pump engineering drives the emergence of frustration-induced quasi-long-range order in a low-dimensional photonic cavity array. We consider a Lieb chain of nonlinear cavities as described by the Bose-Hubbard model and featuring a photonic flat band in the single-particle spectrum. Incoherent pumping of the Lieb lattice leads to a photonic density-wave which manifests an algebraic decay of correlations with twice the period of the lattice unit cell. This work opens up new directions for the emergence of strongly-correlated phases in quantum optical frustrated systems through pump design.

Many-body physics with light is inspired by the combined opportunities offered by quantum optics and condensed matter physics. Superconducting circuits [1] and exciton-polaritons in semiconducting micro-cavities [2] provide platforms for exploring strongly correlated photons with light-matter induced interactions [3, 4]. The inherently nonequilibrium nature of photonic systems adds further opportunities, since the dynamics is not generated by the Hamiltonian alone but rather involves a Liouvillian superoperator acting on the system's density-matrix that incorporates unitary as well as dissipative dynamics. Drive and dissipation then can be tailored to target a desired subspace governing the long-time system dynamics. For instance, reservoir engineering [5] has been demonstrated within various quantum optical settings, e.g., trapped ions [6] and can be utilized in quantum computation [7] or for generating topological phases [8]. Alternatively, exotic many-body states of nonequilibrium systems can be engineered under continuous driving, as recently implemented for entangled steady-states [9, 10] or proposed for fractional quantum Hall states of light [11, 12]. Here, we demonstrate that pump engineering leads to the emergence of quasi-long-range order in a frustrated photonic lattice.

While frustration in equilibrium systems, e.g., in spin lattices [13–15], Josephson junction arrays [16, 17] and ultracold atoms [18–20] has been well explored, only few pioneering efforts have been undertaken in quantum optics [21]. E.g., experiments on frustrated photonic lattices have demonstrated single-particle interference [22, 23], all-optical logical operation using flat band eigenstates [24], and exciton-polariton condensation on a flat band with disorder-induced decoherence [25]. Recently, it has been proposed that a coherently driven frustrated lattice develops an incompressible steady-state [26] characterized by exponentially decaying correlations. Here, we demonstrate that pump engineering allows for the emergence of truly crystalline quasi-long-range order.

We consider a quasi-one-dimensional (1D) Lieb lattice [27] of coupled nonlinear cavities (see Fig. 1) described by the Bose-Hubbard model with Hamiltonian ( $\hbar = 1$ )

$$H = \sum_j \sum_{I=A,B,C} \left[ \omega_I p_{j,I}^\dagger p_{j,I} + U p_{j,I}^\dagger p_{j,I}^\dagger p_{j,I} p_{j,I} \right] + J \sum_j \left[ p_{j,B}^\dagger (p_{j,A} + p_{j,C}) + p_{j+1,B}^\dagger p_{j,C} + \text{H.c.} \right] \quad (1)$$

Here, the bosonic operators  $p_{j,I}^\dagger$  create a photon at site  $I = A, B, C$  in unit cell  $j$  of the Lieb lattice. The first line in the

Hamiltonian (1) contains the on-site energies  $\omega_I$  and Kerr-type interaction  $U$ , while the second line describes photon hopping between nearest-neighbor sites with a rate  $J$ . In the following, we assume  $\omega_A = \omega_C$  and  $\omega_A \neq \omega_B$ . We also set  $\omega_A = 0$  for convenience, while the precise value chosen for  $\omega_B$  does not affect the main results of this paper. The Lieb lattice is originally two-dimensional and is formally obtained from a square lattice by adding a new site at the mid-points of all bonds; when  $\omega_A = \omega_C$  this *decorating procedure* ensures that the band structure of the Lieb lattice exhibits a flat band with energy  $\omega_B = 0$ , i.e., a dispersionless band in the entire Brillouin zone which arises from quantum interference [28]. The lattice considered in our manuscript is a quasi-1D cut of the 2D Lieb lattice that still exhibits a flat band. The flat band is associated with a set of degenerate, single-particle *plaquette* states  $|V_j\rangle$  localized on a compact portion of the lattice,

$$|V_j\rangle = \frac{1}{\sqrt{3}} (p_{j,C}^\dagger - p_{j,A}^\dagger - p_{j+1,A}^\dagger) |\text{vac}\rangle \quad (2)$$

With three sites per unit cell of the quasi-1D Lieb lattice, the single-particle band structure exhibits two more bands with a finite dispersion (see inset in Fig. 2(a)).

The peculiarity of the flat band manifests itself in the many-body problem: starting from the plaquette states (2), exact many-body eigenstates of the Hamiltonian (1) with zero-energy can be constructed from product states of non-overlapping plaquettes, e.g., the two-photon states  $|V_1\rangle |V_3\rangle, |V_1\rangle |V_4\rangle$ , the three-photon states  $|V_1\rangle |V_3\rangle |V_5\rangle$  etc., up to the maximally filled density-wave state

$$|n_{\text{dw}}\rangle = \prod_{j=1}^{n_{\text{dw}}} |V_{2j-1}\rangle \quad (3)$$

whose photon number depends only on the geometry, i.e.,  $n_{\text{dw}} = (N + 1)/2$  for an odd number of unit cells  $N$ , see inset in Fig. 1. The filling is given by  $\nu_{\text{dw}} = n_{\text{dw}}/N_s = 1/6 + \mathcal{O}(1/N)$ , where  $N_s = 3N + 2$  is the number of sites. Products of plaquettes with filling higher than  $\nu_{\text{dw}}$  must double occupy at least one site [18] and are therefore gapped from the zero-energy manifold by a finite interaction energy  $\propto \Delta$ , see Fig. 2(b). The set of flat band states forms a zero-energy manifold with a large degeneracy  $\sum_{n=0}^{n_{\text{dw}}} D_n = F_{2n_{\text{dw}}+1}$ , where  $D_n = \binom{2n_{\text{dw}}-n}{n}$  is the degeneracy of the photon number sector  $n$  and  $F_n$  is the Fibonacci number,  $F_n \sim [(1 + \sqrt{5})/2]^n / \sqrt{5}$  for large  $n$ . Note, that the single-particle plaquette states (2) are linearly independent but not

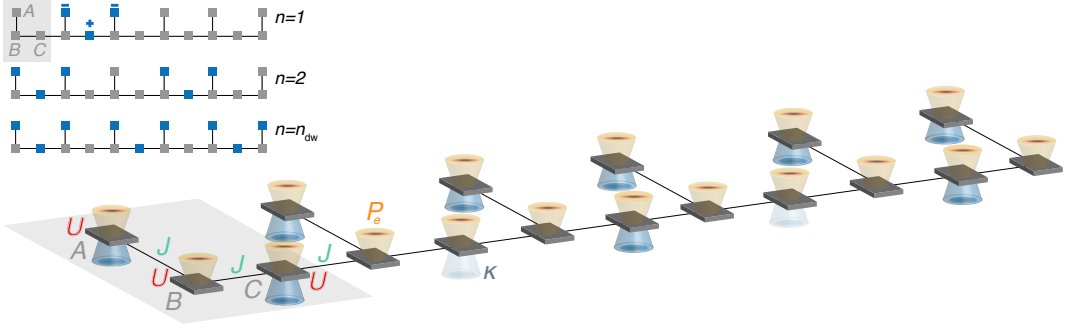


FIG. 1. Schematic view of the pumped and dissipative quasi-one-dimensional Lieb lattice. The lattice has a three-site unit cell with basis sites  $A, B, C$  (grey). Here, the lattice displays  $N = 5$  cells and terminates with  $A$  and  $C$  sites for symmetry. Photons can hop between neighboring sites with amplitude  $J$  (green) and experience an on-site repulsion  $U$  (red), as described by the Bose-Hubbard Hamiltonian, see equation (1). The Lieb lattice hosts a set of single-particle (photon number  $n = 1$ ) plaquette states localized on one  $C$  site and two neighboring  $A$  sites (top-left inset); these originate from destructive quantum interference of amplitudes at site  $A$ , see equation (2). Product states of non-overlapping plaquettes are many-body eigenstates of the Hamiltonian with zero interaction energy. The lattice is pumped homogeneously with strength  $P_e$  (orange light cones) and loses photons to the environment with a rate  $\kappa$ . The nonequilibrium dynamics is described by the master equation (4). Due to the energy-dependent spectral density of the pump, the steady-state is a density-wave where only every second  $C$  site is occupied (blue light cones) giving rise to frustration-induced quasi-long-range order, see equation (7).

orthogonal since neighboring plaquettes share one site; we thus perform a Gram-Schmidt orthogonalization of the flat-band manifold in each excitation sector separately, since states with different excitation numbers are orthogonal, see Supplemental Material (SM).

The density-wave (3) exhibits strong density correlations with a period twice that of the lattice (period doubling) since only every second  $C$  site is occupied, thus representing a truly crystalline state. There have been much efforts lately towards the implementation of strongly-correlated states in frustrated system, originally in the context of ultracold atoms [18, 29] and more recently in quantum optical systems [22–26]. In the former (equilibrium) case, the task is highly nontrivial since the flat band is not the lowest energy band and a fully adiabatic transfer of the condensate would be required [29]. Alternatively, in frustrated lattices of similar kind, e.g., the sawtooth chain or the kagome lattice where the flat band is the topmost energy band, equilibrium frustration can be investigated only through band inversion, e.g. by implementing complex-valued tunnelling constants [30]. In nonequilibrium photonic systems, coherent driving allows to populate the flat band manifold [22, 23] but leads to a mixed steady-state with weak occupation of the density-wave [26].

Here, we propose a radically different route which allows to engineer a quasi-pure density-wave exhibiting an algebraic decay of photonic density-density correlations. To this end, the Lieb chain is incoherently coupled to an external pump reservoir exhibiting a Lorentzian-shaped spectral density centered at zero energy. This coloured environment can be engineered, e.g., in circuit QED using microwave filters [31] or ancilla quantum systems [32]. The dynamics of the system is then described by a time-convolutionless master equation in the Born approximation [31–33] for the lattice density matrix

$$\dot{\rho} = i[\rho, H] + (\kappa/2) \sum_{j,I} \mathcal{L}_{j,I}^{\downarrow}[\rho] + (P_e/2) \sum_{j,I} \mathcal{L}_{j,I}^{\uparrow}[\rho]. \quad (4)$$

Here, we have introduced the Lindblad dissipators  $\mathcal{L}_{j,I}^{\downarrow}[\rho] = 2p_{j,I}\rho p_{j,I}^{\dagger} - p_{j,I}^{\dagger}p_{j,I}\rho - \rho p_{j,I}^{\dagger}p_{j,I}$  and the generalized superoperators  $\mathcal{L}_{j,I}^{\uparrow}[\rho] = p_{j,I}^{\dagger}\rho \tilde{p}_{j,I} - \rho \tilde{p}_{j,I}p_{j,I}^{\dagger} + \text{H.c.}$  The first term in equation (4) describes the coherent evolution under the lattice Hamiltonian  $H$ , the second accounts for photon loss from each site with a rate  $\kappa$ , and the last term stands for an energy dependent incoherent pump with strength  $P_e$ . The energy dependence is encoded in the generalized operators  $\tilde{p}_{j,I} = \sum_{n,\alpha,\alpha'} S_{n-1\alpha',n\alpha} \langle n-1, \alpha' | p_{j,I} | n, \alpha \rangle | n-1, \alpha' \rangle \langle n, \alpha |$ , which are expressed in the eigenbasis  $H | n, \alpha \rangle = \omega_{n,\alpha} | n, \alpha \rangle$  with eigenenergies  $\omega_{n,\alpha}$ . Here, the index  $\alpha$  labels the states for a given photon number  $n$ . The jump operators  $\tilde{p}_{j,I}$  induce transitions between different eigenstates of  $H$  with a probability determined by the spectral weight of the reservoir

$$S_{n-1\alpha',n\alpha} = \frac{\Gamma/2}{-i(\omega_{n,\alpha} - \omega_{n-1,\alpha'} - \omega_s) + \Gamma/2} \quad (5)$$

The latter is Lorentzian-shaped with a width  $\Gamma$  (see Fig. 2(a)). Note, that for a white noise bath ( $\Gamma \rightarrow \infty$ ) one recovers a standard Lindblad term with  $\tilde{p}_j \rightarrow p_j$ .

We now show that one can engineer a quasi-pure steady-state by carefully designing the parameters of the pump. In particular, it is the spectral weight  $S_{n-1\alpha',n\alpha}$  which determines the eigenstates that are mostly populated by the drive. Centering the spectral profile (5) at zero energy, i.e.,  $\omega_s = 0$ , implies that as long as the width  $\Gamma$  and the strength  $P_e$  are sufficiently small ( $\Gamma, P_e < \Delta$ ), only the (flat) zero-energy manifold is effectively pumped by the reservoir. In this case, we project the density matrix on the flat band manifold selected by the projector  $\mathcal{P} = |\text{vac}\rangle \langle \text{vac}| + \dots + |n_{\text{dw}}\rangle \langle n_{\text{dw}}|$  and  $\rho \approx \mathcal{P}\rho\mathcal{P}$ . In this flat band eigenspace, we solve the master equation (4) analytically (see SM). The density matrix then is a diagonal mixture of flat band eigenstates with occupation

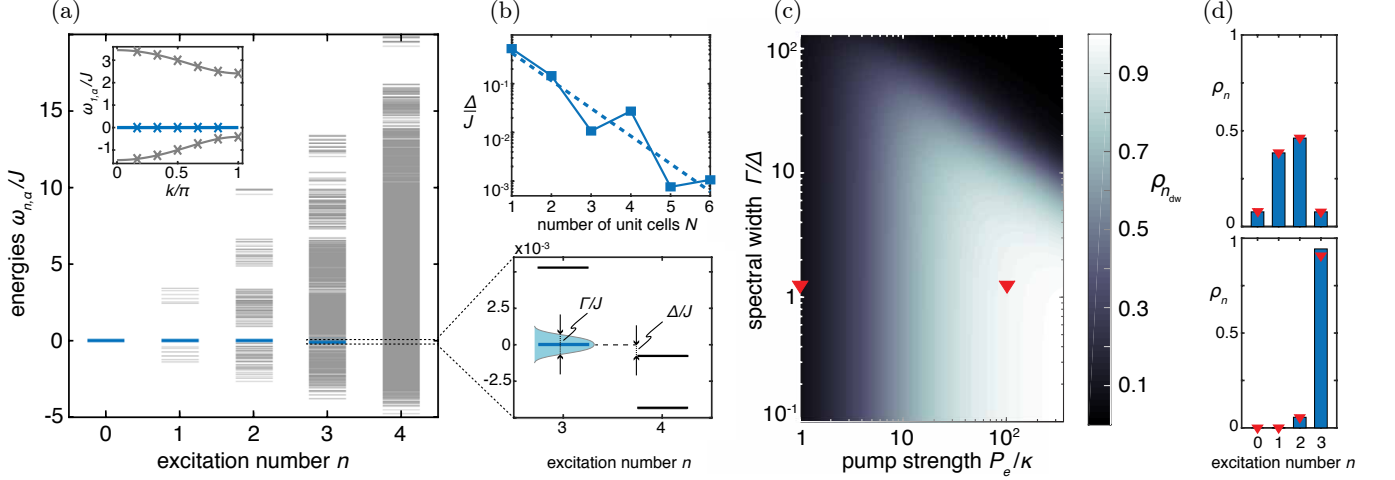


FIG. 2. (a) Energy levels  $\omega_{n,\alpha}/J$  of the quasi-1D Lieb lattice (1) with  $N=5$  unit cells, i.e.,  $3N+2$  sites, as a function of excitation (photon) number  $n$ , while the index  $\alpha$  labels energies at fixed  $n$ . The levels  $\omega_{n,\alpha}$  are scaled to the hopping amplitude  $J$  and have been obtained via exact diagonalization (see SM). Frustration in the Lieb chain leads to a set of single-particle ( $n=1$ ) plaquette states at zero-energy, see equation (2); product states of non-overlapping plaquettes are also zero-energy eigenstates with  $n > 1$  up to the density-wave state, see equation (3), with  $n_{\text{dw}} = (N+1)/2$ , i.e.,  $n_{\text{dw}} = 3$  in (a). This manifold is marked by the blue lines (including the vacuum with  $n=0$ ). The top-left inset shows the single-particle levels  $\omega_{n=1,\alpha}$  in momentum space (crosses), including lines for large  $N$  (note the zero-energy flat band). The band structure asymmetry is due to a finite offset  $\omega_A \neq \omega_B$ . (b) The zero-energy manifold is pumped (see text) using a Lorentzian spectral density. Occupation of other levels is suppressed if the width  $\Gamma$  is smaller than the minimal excitation gap  $\Delta$  to higher bands with  $n = n_{\text{dw}} + 1$  (bottom panel). The gap decreases with system size, see top panel in (b). The dashed line is an exponential fit,  $\Delta/J \propto \exp(-\gamma N)$ ,  $\gamma = 1.31 \pm 0.67$ . (c) Occupation of the density-wave  $\rho_{n_{\text{dw}}}$  from the numerical solution of the master equation (4) as a function of the Lorentzian width  $\Gamma/\Delta$  and pump strength  $P_e/\kappa$  for the lattice with  $N=5$  unit cells as in (a). For small  $\Gamma$  and large  $P_e$  the steady-state of the Lieb chain is a quasi-pure density-wave. (d) Populations within the flat band manifold, as obtained from the analytical solution of the master equation (4) in the projected Hilbert space (6) (bars), versus numerical results (symbols), for  $\Gamma/\Delta = 1.3$  and  $P_e/\kappa = 1$  (top) and  $P_e/\kappa = 10^2$  (bottom, cf. points marked by triangles in (c)) showing excellent agreement supporting the validity of the analytic study. The other parameters are chosen as,  $U/J = 2.5$ ,  $\kappa/\Gamma = 10^{-3}$ ,  $\omega_B = \omega_A + 2J$ .

probabilities given by

$$\frac{\rho_n}{\rho_{n_{\text{dw}}}} = D_n \left( \frac{\kappa}{P_e} \right)^{n_{\text{dw}} - n} \quad (6)$$

where  $\rho_n$  is the population of the manifold with  $n$  photons in the flat band,  $\rho_n = \sum_{\alpha} \rho_{n,\alpha}$ ,  $\rho_{n,\alpha} = \langle n, \alpha | \rho | n, \alpha \rangle$  with  $n = 0, \dots, n_{\text{dw}}$ . Consequently, when  $P_e \gg \kappa$ , we find  $\rho \approx |n_{\text{dw}}\rangle \langle n_{\text{dw}}| + \mathcal{O}(\kappa/P_e)$ , i.e., a quasi-pure density-wave state.

In order to check the validity of this analytic result, we solve the master equation numerically in the full lattice Hilbert space using a block diagonalization algorithm (see SM). We consider a finite-size system with  $N=5$  unit cells, i.e.,  $N_s = 17$  sites, corresponding to a density-wave with  $n_{\text{dw}} = 3$ . Figs. 2(c,d) show the population of the density-wave state  $\rho_{n_{\text{dw}}}$  in a colour-scale map as a function of the Lorentzian width  $\Gamma/\Delta$  and pump strength  $P_e/\kappa$ . Indeed, we obtain an almost pure density wave state if two conditions are fulfilled: (i) The spectral width and the strength of the reservoir are smaller than the excitation gap ( $\Gamma, P_e < \Delta$ ) such that only flat band states are effectively excited; (ii) the pump strength is larger than the dissipation rate ( $P_e \gg \kappa$ ) such that the density wave state has the largest population among all flat band states.

It is the analysis of the spatial correlations which brings forward the key properties of this interesting nonequilibrium steady-state. We determine the density-density

correlator (second-order coherence of the electromagnetic field) emitted by the  $C$  sites in the lattice, i.e.,  $g_{i,j}^{(2)} = \langle p_{i,c}^\dagger p_{j,c}^\dagger p_{i,c} p_{j,c} \rangle / (\langle p_{i,c}^\dagger p_{i,c} \rangle \langle p_{j,c}^\dagger p_{j,c} \rangle)$ . Fig. 3(a) shows the spatial correlations of the first  $C$  site ( $i=1$ ) with its neighbors as obtained from the solution of the master equation in the projected Hilbert space (line) for a lattice with  $N=15$  unit cells. Remarkably, we find extended density-wave oscillations whose envelope (dashed) decays algebraically,

$$g_{1,2j}^{(2)} = 1 - 1/j^\beta + \mathcal{O}[(\kappa/P_e)^2] \quad (7)$$

Equation (7) marks the appearance of double-periodic quasi-long-range order in this system and is the central result of our paper, i.e., a truly crystalline state of light, induced by frustration and pump engineering. Making use of a log-log linear-regression fit and extrapolating to  $N \rightarrow \infty$  (inset in Fig. 3(a)), we find  $\beta = 1.05 \pm 0.02$ . This estimate is consistent with the analytic solution to first order in  $\kappa/P_e$  (see SM), which yields  $\beta = 1$ . This result is also compared with exact simulations for a smaller lattice with  $N=7$  unit cells and excellent agreement is obtained. The crystalline state of light is further characterized by a geometric filling factor of  $\nu = n_{\text{dw}}/N_s \approx 1/6$  and vanishing compressibility as shown in Fig. 3(b) (see Figure caption for a more detailed discussion). We note that a different mechanism for achieving long-range crystalline order based on the combination of electromagnetically induced

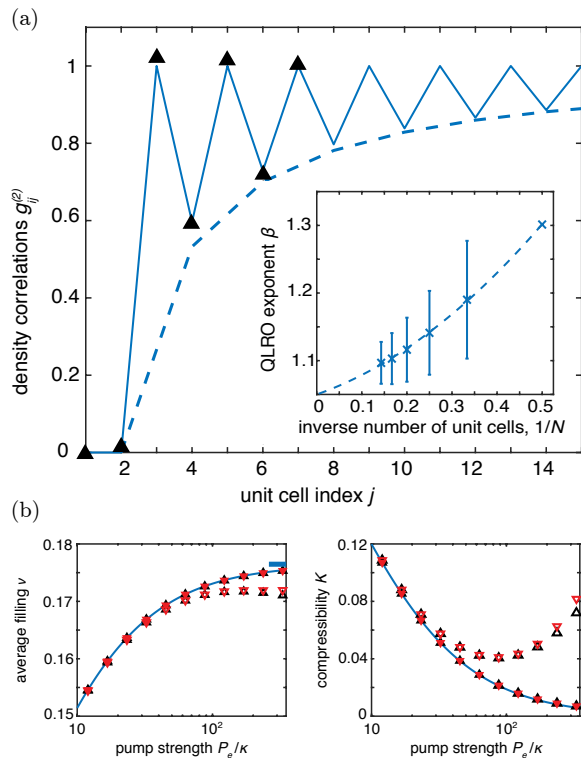


FIG. 3. (a) Density-density correlator of  $C$  sites  $g_{i,j}^{(2)}$  showing quasi-long-range order (QLRO). The result obtained from the projected Hilbert space for a lattice with  $N = 15$  unit cells (line) agrees well with the exact numerics for a smaller system of  $N = 7$  unit cells (symbols). The pump strength is  $P_e/\kappa = 75$  and we have chosen  $\Gamma/\Delta = 1.5$  in our numerical analysis, with  $\Delta/J \approx 3 \times 10^{-4}$  the excitation gap for  $N = 7$ . The fitted envelope of the density-wave oscillations (dashed) decays algebraically with an exponent  $\beta$  (inset). (b) Average filling  $\nu = \bar{n}/N_s$  (left) and compressibility  $K = (\sum_n n^2 \rho_n - \bar{n}^2)/\bar{n}$  (right) as a function of pump strength  $P_e/\kappa$  for fixed values of the Lorentzian width  $\Gamma/\Delta = 0.13, 1.3$ . Here,  $\bar{n} = \sum_n n \rho_n$  denotes the population of the manifold with photon number  $n$  and  $\rho_n = \sum_\alpha \rho_{n,\alpha}$ . The analytical solution of the master equation (4) in the projected Hilbert space (6) (lines) agrees well with the exact numerics for small values of the Lorentzian width  $\Gamma/\Delta = 0.13$  (filled symbols, on top of the line). Deviations occur when the spectral width  $\Gamma/\Delta = 1.3$  (open symbols) is comparable with the excitation gap (see Fig. 2) at large pump strengths. The black upward (red downward) triangles are obtained including up to  $n = n_{\text{dw}} + 1$  ( $n = n_{\text{dw}} + 2$ ) excitations in the full lattice Hilbert space, with good convergence obtained in the data.

transparency and dipolar interactions between Rydberg polaritons was also proposed in [34, 35].

We now provide an estimate of the parameters for a proof-of-principle implementation using circuit QED, i.e., nonlinear microwave resonators, which are coupled capacitively to each other [1]. In the dispersive regime of circuit QED [31], a Kerr nonlinearity  $U \approx 2$  MHz, inter-cavity coupling strength  $J \approx 200$  MHz and a cavity decay rate  $\kappa \approx 5$  kHz are readily achievable with current technology [1]. In order to engineer one period of a density-wave, we need at least  $N = 4$  unit cells with  $n_{\text{dw}} = 2$ . For this system size and parameters,

the minimal excitation gap would be  $\Delta \approx 0.001J \approx 2$  MHz (calculated as in Fig. 2b). In order to stay in the small bandwidth ( $\Gamma, P_e < \Delta$ ) and strong pump regime ( $P_e \gg \kappa$ ), we can choose  $\Gamma \sim 1$  MHz and  $P_e \sim 100$  kHz. Going to extended arrays of superconducting qubits with stronger Kerr nonlinearities would allow for a large-scale realization of our proposal [36]. An alternative platform for the implementation of the photonic density-wave are exciton-polaritons in semiconducting microcavities, where a Lieb chain has already been engineered [25].

An interesting question for future work concerns the strong pump regime, where dispersive states become significantly occupied and density-wave oscillations are expected to vanish. In equilibrium, the density-wave state is destroyed by particle doping in the quasi-1D sawtooth chain but survives together with superfluidity in the 2D kagome lattice giving rise to a supersolid phase [18]. Whether such a picture remains valid out of equilibrium is an open question, with the potential for the discovery of novel photonic phases. An equally interesting direction concerns the nonequilibrium many-body system in the presence of disorder, given that the single-particle eigenstates become critical when the dispersive band and the flat band touch, e.g., in the 2D Lieb or kagome lattice [37, 38].

## SUPPLEMENTAL MATERIAL

*Flat band projection.* The flat band manifold is given by the set of all noninteracting (non-overlapping) flat band states that can be written starting from the single-particle plaquette states (2), i.e., the single excitation (photon) states  $|1, \alpha\rangle = |V_1\rangle, |V_2\rangle$  etc., the two-photon states  $|2, \alpha\rangle = |V_1\rangle |V_3\rangle, |V_1\rangle |V_4\rangle$  etc., the three-photon states  $|3, \alpha\rangle = |V_1\rangle |V_3\rangle |V_5\rangle, |V_1\rangle |V_3\rangle |V_6\rangle$  etc., up to the maximally excited density-wave state  $|n_{\text{dw}}\rangle$  in (3), with the addition of the vacuum state  $|0\rangle = |\text{vac}\rangle$  as well. Here,  $\alpha$  labels the flat band eigenstates within each excitation number sector  $n$  with degeneracy  $D_n = \binom{2n_{\text{dw}} - n}{n}$ . Note that the sectors with  $n = 0, n_{\text{dw}}$  are special with  $D_0 = D_{n_{\text{dw}}} = 1$ . The entire set forms the macroscopically degenerate zero-energy manifold with degeneracy  $F_{2n_{\text{dw}}+1}$  discussed in the main text. Note, that the single-particle plaquette states (2) are linearly independent but not orthogonal since neighboring plaquettes share one site. We thus perform (numerically) a Gram-Schmidt orthogonalization of the  $|n, \alpha\rangle$  for each  $n$  to obtain the orthogonalized new basis  $|n, \alpha\rangle_o$ . The orthogonalization procedure allows to construct the projector

$$\mathcal{P} = \sum_{n=0}^{n_{\text{dw}}} \sum_{\alpha=1}^{D_n} |n, \alpha\rangle_o \langle n, \alpha| \quad (8)$$

which we use to project the density matrix  $\mathcal{P}\rho\mathcal{P}$  and the operators  $\mathcal{P}p_j\mathcal{P}$ . The master equation then reduces to a rate equation for the populations of the flat band states (the diagonal entries of the density matrix), which can be solved analytically, see equation (10) below. The solution for the populations in (6) does not depend on the orthogonalization, while the correlator  $g_{i,j}^2$  in (7) does, since it is determined by the spatial

structure of the eigenstates.

*Exact diagonalization.* We diagonalize the Hamiltonian (1) in each excitation number sector separately to obtain a complete basis  $|n, \alpha\rangle$ ,  $H|n, \alpha\rangle = \omega_{n,\alpha}|n, \alpha\rangle$ . Here,  $\alpha$  labels all states in the excitation number sector  $n$ , see e.g. Fig. 2(a). We then write the master equation (4) in this eigenbasis and obtain a rate equation for the populations  $\rho_{n,\alpha} = \langle n, \alpha | \rho | n, \alpha \rangle$ , i.e.,

$$\dot{\rho}_{n,\alpha} = \sum_{\alpha'} \left[ \kappa G_{n,\alpha,\alpha'} \rho_{n+1,\alpha'} + P_e \tilde{G}_{n,\alpha,\alpha'} \rho_{n-1,\alpha'} \right] - \rho_{n,\alpha} (\kappa W_{n,\alpha} + P_e \tilde{W}_{n,\alpha}) \quad (9)$$

with  $G_{n,\alpha,\alpha'} = \sum_{j,I} \langle n, \alpha | p_{j,I} | n+1, \alpha' \rangle^2$ ,  $\tilde{G}_{n,\alpha,\alpha'} = \text{Re}[S_{n\alpha, n-1\alpha'}] \sum_{j,I} |\langle n, \alpha | p_{j,I}^\dagger | n-1, \alpha' \rangle|^2$ ,  $W_{n,\alpha} = \sum_{j,I} \langle n, \alpha | p_{j,I}^\dagger p_{j,I} | n, \alpha \rangle$  and  $\tilde{W}_{n,\alpha} = \sum_{\alpha'} \tilde{G}_{n+1,\alpha',\alpha}$ . The first two terms in equation (9) describe the incoherent excitation of level  $n$  due to losses from level  $n+1$  and pump from level  $n-1$ , while the last two terms describe the corresponding losses out of the sector  $n$ . Solving the rate equations allows to circumvent the computational costs of the master equation, since we only need to obtain the diagonal entries of  $\rho$ . This approach allows to analyze lattice sizes of the order of 20 sites, i.e., Hilbert spaces with  $> 10^6$  states. Such system sizes are typically far beyond exact diagonalization methods (note, that tensor network approaches are not directly applicable here since a matrix representation of the generalized operators  $\tilde{p}_j$  requires to first solve for the complete eigenbasis of  $H$ , i.e., including the excited states). The rate equation (9) is solved numerically imposing a cutoff in the number of photons per site  $n_{\text{loc}}$  and a global cutoff in the number of excitations in the lattice  $n_{\text{glob}}$ . We then verify convergence in these truncation parameters. All converged results shown are obtained using up to  $n_{\text{loc}} = 2$  and  $n_{\text{glob}} = 5$ .

*Rate equation in the projected Hilbert space.* For flat band states, the rate equation (9) simplifies greatly, since  $S_{n-1\alpha', n\alpha} = 1$ ,  $\sum_{\alpha} G_{n,\alpha,\alpha'} = n+1$ ,  $\sum_{\alpha'} \tilde{G}_{n,\alpha,\alpha'} = n$ ,

$W_{n,\alpha} = n$  and  $\sum_{\alpha} \tilde{W}_{n,\alpha} = (n+1)D_{n+1}$ . Summing over  $\alpha$  in equation (9), one finds

$$\dot{\rho}_n = \kappa(n+1)\rho_{n+1} + P_e n \frac{D_n}{D_{n-1}} \rho_{n-1} - \kappa n \rho_n - P_e(n+1) \frac{D_{n+1}}{D_n} \rho_n \quad (10)$$

with  $\rho_n = \sum_{\alpha} \rho_{n,\alpha}$  and  $n = 0, \dots, n_{\text{dw}}$ . The solution is easily determined analytically,

$$\frac{\rho_{n+1}}{\rho_n} = \frac{P_e D_{n+1}}{\kappa D_n} \quad (11)$$

from which we obtain the expression (6).

*Density-density correlator in the projected Hilbert space.* In the strong pumping regime  $P_e \gg \kappa$ , the density matrix takes the form  $\rho \approx |n_{\text{dw}}\rangle \langle n_{\text{dw}}| + (\kappa/P_e) \sum_{\alpha \in D_{n_{\text{dw}}-1}} |n, \alpha\rangle \langle n, \alpha| + \mathcal{O}[(\kappa/P_e)^2]$ . The correlator  $g_{i,j}^{(2)} = \langle p_{i,c}^\dagger p_{j,c}^\dagger p_{i,c} p_{j,c} \rangle / (\langle p_{i,c}^\dagger p_{i,c} \rangle \langle p_{j,c}^\dagger p_{j,c} \rangle)$  is calculated using the formula  $\langle O \rangle = \text{Tr}[\rho O] / \text{Tr}[\rho]$ . It is straightforward to show that  $g_{1,2j+1}^{(2)} = 1 + \mathcal{O}[(\kappa/P_e)^2]$  since the expectation values are dominated by the density-wave contribution to the density matrix. Here,  $j = 1, \dots, (N-1)/2$ , while  $g_{1,1}^{(2)} = 0$  trivially. Calculation of the correlator  $g_{1,2j}^{(2)}$ ,  $j = 1, \dots, (N-1)/2$  is more involved and the contribution of the manifold below the density-wave, i.e., with  $n = n_{\text{dw}} - 1$ , must be taken into account. Neglecting the orthogonalization of the states in this manifold, we find  $g_{1,2j}^{(2)} = 1 - 1/j + \mathcal{O}[(\kappa/P_e)^2]$ .

## ACKNOWLEDGEMENTS

We thank I. Carusotto, E.P.L. v. Nieuwenburg and H.E. Türeci for discussions and acknowledge support from the Swiss National Science Foundation through the National Centre of Competence in Research ‘QSIT–Quantum Science and Technology’ (MB).

- 
- [1] Schmidt, S. & Koch, J. Circuit QED lattices: Towards quantum simulation with superconducting circuits. *Ann. der Physik* **525**, 395–412 (2013).
- [2] Carusotto I. & Ciuti, C. Quantum fluids of light. *Rev. Mod. Phys.* **85**, 299–366 (2013).
- [3] Hartmann, M.J. Quantum simulation with interacting photons. *J. Opt.* **18**, 104005 (2016).
- [4] Noh, C. & Angelakis, D.G. Quantum simulations and many-body physics with light. *Rep. Prog. Phys.* **80**, 016401 (2017).
- [5] Cirac, J.I., Parkins, A.S., Blatt, R. & Zoller, P. *Phys. Rev. Lett.* **70**, 556–559 (1993).
- [6] Kienzler, D. *et al.* Quantum harmonic oscillator state synthesis by reservoir engineering. *Science* **347**, 53–56 (2015).
- [7] Verstraete, F., Wolf, M.M. & Cirac, J.I. Quantum computation and quantum-state engineering driven by dissipation. *Nature Phys.* **5**, 633–636 (2009).
- [8] Diehl, S., Rico, E., Baranov, M.A. & Zoller, P. Topology by dissipation in atomic quantum wires. *Nature Phys.* **7**, 971–977 (2011).
- [9] Lin, Y. *et al.* Dissipative production of a maximally entangled steady state of two quantum bits. *Nature* **504**, 415–418 (2013).
- [10] Shankar, S. *et al.* Autonomously stabilized entanglement between two superconducting quantum bits. *Nature* **504**, 419–422 (2013).
- [11] Kapit, E., Hafezi, M. & Simon, S.H. Induced self-stabilization in fractional Quantum Hall states of light. *Phys. Rev. X* **4**, 031039 (2014).
- [12] Umucalilar, R. O. & Carusotto, I. Generation and spectroscopic signatures of a fractional quantum Hall liquid of photons in an incoherently pumped optical cavity. *Phys. Rev. A* **96**, 053808

- (2017).
- [13] Castelnovo, C., Moessner, M., Sondhi, S.L. Magnetic monopoles in spin ice. *Nature* **451**, 42–45 (2008).
- [14] Villain, J., Bidaux, R., Carton, J.-P., & Conte, R. Order as an effect of disorder, *J. Phys. France* **41**, 1263–1272 (1980).
- [15] Bergman, D., Alicea, J., Gull, E., Trebst, S. & Balents, L. Order-by-disorder and spiral spin-liquid in frustrated diamond-lattice antiferromagnets. *Nature Phys.* **3**, 487–491 (2007).
- [16] Pannetier, B., Chaussy, J., Rammal, R., & Villegier, J.C. Experimental fine tuning of frustration: two-dimensional superconducting network in a magnetic field, *Phys. Rev. Lett.* **53**, 1845 (1984).
- [17] Vidal, J., Mosseri, R., & Douçot, B. Aharonov-Bohm Cages in Two-Dimensional Structures, *Phys. Rev. Lett.* **81**, 5888 (1998).
- [18] Huber, S.D. & Altman E., Bose condensation in flat bands. *Phys. Rev. B* **82**, 184502 (2010).
- [19] Apaja, V., Hyrkäs, M. & Manninen, M. Flat bands, Dirac cones, and atom dynamics in an optical lattice. *Phys. Rev. A*, **82**, 041402 (2010).
- [20] Tovmasyan, M., van Nieuwenburg, E.P.L. & Huber, S.D. Geometry-induced pair condensation. *Phys. Rev. B* **88**, 220510 (2013).
- [21] Schmidt, S. Frustrated polaritons. *Phys. Scr.* **91**, 073006 (2016).
- [22] Vicencio, R. *et al.* Observation of localized states in Lieb photonic lattices. *Phys. Rev. Lett.* **114**, 245503 (2015).
- [23] Mukherjee, S. *et al.* Observation of a localized flat-band state in a photonic Lieb lattice. *Phys. Rev. Lett.* **114**, 245504 (2015).
- [24] Real, B. *et al.* Flat-band light dynamics in Stub photonic lattices. *Sci. Rep.* **7**, 15085 (2017)
- [25] Baboux, F. *et al.* Bosonic condensation and disorder-induced localization in a flat band. *Phys. Rev. Lett.* **116**, 066402 (2016).
- [26] Biondi, M., van Nieuwenburg, E.P.L., Blatter, G., Huber, S.D. & Schmidt, S. Incompressible polaritons in a flat band. *Phys. Rev. Lett.* **115**, 143601 (2015).
- [27] Lieb, E. H. Two theorems on the Hubbard model. *Phys. Rev. Lett.* **62**, 1201 (1989).
- [28] Tasaki, H. Ferromagnetism in the Hubbard models with degenerate single-electron ground states. *Phys. Rev. Lett.* **69**, 1608 (1992).
- [29] Taie, S. *et al.* Coherent driving and freezing of bosonic matter wave in an optical Lieb lattice. *Sci. Adv.* **1**, e1500854 (2015).
- [30] Aidelsburger, M. *et al.* Measuring the Chern number of Hofstadter bands with ultracold bosonic atoms. *Nature Phys.* **11**, 162–166 (2015).
- [31] Hoffman, A.J. *et al.* Dispersive photon blockade in a superconducting circuit. *Phys. Rev. Lett.* **107**, 053602 (2011).
- [32] Lebrenilly, J., Wouters, M. & Carusotto, I. Towards strongly correlated photons in arrays of dissipative nonlinear cavities under a frequency-dependent incoherent pumping. *C. R. Physique* **17**, 836–860 (2016).
- [33] Breuer, H.-P. & Petruccione, F. *The Theory of Open Quantum Systems* (Oxford, 2002).
- [34] Chang, D.E. *et al.* Crystallization of strongly interacting photons in a nonlinear optical fibre. *Nature Phys.* **4**, 884–889 (2008).
- [35] Otterbach, J., Moos, M., Muth, D., & Fleischhauer, M. Wigner crystallization of single photons in cold Rydberg ensembles. *Phys. Rev. Lett.* **111**, 113001 (2013).
- [36] Neill, C. *et al.* A blueprint for demonstrating quantum supremacy with superconducting qubits. arXiv:1709.06678, (2017).
- [37] Chalker, J.T, Pickles, T.S. & Shukla, P. Anderson localization in tight-binding models with flat bands. *Phys. Rev. B* **82**, 104209 (2010).
- [38] Leykam, D., Flach, S., Bahat-Treidel, O., & Desyatnikov, A.S. Flat band states: Disorder and nonlinearity. *Phys. Rev. B* **88**, 224203 (2013).